Flexible Demand Through Point-of-Load Voltage Control in Domestic Sector

Jinrui Guo, *Student Member, IEEE*, Balarko Chaudhuri, *Senior Member, IEEE*, and Shu Yuen Ron Hui, *Fellow, IEEE*

***Abstract*—Demand reduction through voltage control at substations (VCSs) is commonly used. However, during high loading conditions the allowable depth of voltage reduction could be limited by the large voltage drop across the feeders. Distributed voltage control at the points of connection of individual loads (e.g., supply point of a cluster of domestic customers) allows larger flexibility in demand, especially during high loading as demonstrated in this paper. A high-resolution stochastic demand model and the aggregate power-voltage sensitivity of individual domestic customers are used to compare the demand reduction capability of point-of-load voltage control (PVC) against VCS. The rating of the voltage compensators required for PVC is evaluated to weigh the benefits against the required investment. First, the results are shown on a generic low voltage network with random distribution of clusters of domestic customers at various buses and random length of feeder segments to draw general conclusions. Then, the Cigre benchmark medium- and low-voltage networks are used to substantiate the findings. A case study on an islanded microgrid is presented to show that PVC reduces frequency variations caused by fluctuating wind power generation.**

***Index Terms*—Demand response, voltage control, flexible demand, distribution network, microgrid, frequency control.**

List of Acronyms and Notations

Acronyms

DR	Demand reduction
CDC	Cluster of domestic customers
PVC	Point-of-load voltage control
VCS	Voltage control at substation
GVC	Generator voltage control
PEC	Power electronic compensators
DPD	Diversified peak demand
UB, LB	Upper, Lower boundary.

Notations

P, Q	Aggregate active/reactive power per CDC
n_p, n_q	Aggregate active/reactive power-voltage sensitivity per CDC
N_c	Number of CDCs
V_S	Substation voltage
V_B, V_B'	Feeder-side voltage before/after DR
V_C	Voltage injected by the PEC
P_T	Total DPD at nominal voltage
R_T	Total feeder resistance
ΔP_{LL}	Change in network power loss after DR
P_{LC}	Power loss incurred in the PEC
S_C	Apparent power processed by the PEC
DR_{VCS}	DR capability using VCS
DR_{PVC}	DR capability using PVC
P_h	Aggregate active power per domestic customer
n_{ph}	Aggregate active power-voltage sensitivity per domestic customer
N_h	Number of domestic customers within a CDC
P_d	Active power per appliance
Z_p, I_p, P_p	ZIP load model coefficients for appliances.

Manuscript received April 9, 2018; revised July 6, 2018; accepted August 14, 2018. Date of publication August 23, 2018; date of current version June 19, 2019. This work was supported in part by the Engineering and Physical Science Research Council, U.K., under Grant EP/K036327/1, in part by the Hong Kong Research Grant Council through the Theme-Based Project under Grant T23-701/14-N, and in part by the China Scholarship Council and Imperial College London under Grant 201604100122. Paper no. TSG-00538-2018. *(Corresponding author: Jinrui Guo.)*

J. Guo and B. Chaudhuri are with the Department of Electrical and Electronic Engineering, Imperial College London, London SW7 2AZ, U.K. (e-mail: j.guo16@imperial.ac.uk; b.chaudhuri@imperial.ac.uk).

S. Y. R. Hui is with the Department of Electrical and Electronic Engineering, Imperial College London, London SW7 2AZ, U.K., and also with the Department of Electrical and Electronic Engineering, University of Hong Kong, Hong Kong (e-mail: r.hui@imperial.ac.uk).

Color versions of one or more of the figures in this paper are available online at http://ieeexplore.ieee.org.

Digital Object Identifier 10.1109/TSG.2018.2866369

I. Introduction

DECARBONISATION of the electricity supply sector would require integration of large amounts of intermittent renewable energy sources (e.g., wind and solar power) into the electric power networks. Balancing the supply and demand would be a major challenge necessitating larger amount of operating reserve from energy storage, demand reduction etc.

Flexibility in demand is commonly associated with operating the deferrable loads (e.g., washing machine, dish washer etc.) during hours of low electricity demand (i.e., low electricity price) [1] and altering the power consumption of thermostatically controlled loads (e.g., fridges, air-conditioners etc.) without noticeable impact on the consumers [2]. Another way to harness demand flexibility is to utilize the voltage dependence of loads for peak demand reduction (for example) by decreasing the operating voltage of the distribution feeders [3]. Recently, Electricity North West Limited in Great Britain has conducted field trials to manage the load power consumption through feeder voltage reduction [4]. This is exercised through transformer tap changer control at the substation with appropriate line drop compensation. However,

during high loading conditions, the depth of allowable voltage reduction could be limited due to large voltage drop across the feeders so that the voltages at the far end can be maintained within the stipulated limits. Shunt reactive compensation would have limited effect on flattening the voltage profile in low-voltage (LV) feeders. With increasing loading this could seriously limit the demand reduction (DR) capability through voltage control at substation (VCS) alone. Moreover, conventional volt-var measures lack the flexibility to effectively deal with the volatility resulting from large renewable penetration [5].

Provision of voltage control at the points of connection of individual loads (e.g., supply point of a cluster of domestic customers) along the length of a feeder is likely to allow higher DR compared to VCS. However, the capital investment in mass deployment of the voltage compensators for point-of-load voltage control (PVC) should be considered carefully against the benefits. This is especially true for power electronic compensators (PEC) which provide faster control and can handle high volatility. A comparison between the DR capability of PVC against VCS is yet to be reported which motivates this paper. For PVC, a PEC could decouple a cluster of domestic customers (CDC) from the low voltage (LV) feeder so that the supply voltage to each CDC could be controlled individually within the stipulated limits. Aggregated voltage dependence of all the domestic loads could thus be 'fully' exploited. The PEC would be fractionally rated as it is installed in series between the feeder and the CDC.

PVC using Electric Springs [6] has been reported for voltage regulation [7], [8], grid frequency control [9] and power quality improvement [10]. These papers have mostly assumed impedance-type loads without accounting for the time-varying incidence of various loads over a 24-hour period. In [11], different types of loads were used without considering the time-varying incidence of various loads throughout a day. A methodology for estimating the hourly variation of available reserve with PVC was reported in [12] using load disaggregation at the bulk supply point but without considering the distribution network explicitly. In practice, it is critical for the network operators to know the DR capability of PVC during different time of the day so that they can schedule the conventional operating reserve accordingly.

Previous work on quantification of voltage driven DR capability with VCS employed aggregate load models at the medium voltage (MV) level which includes the influence of medium- and low-voltage (MV/LV) network components [4]. These models are not suitable for analysis of DR with PVC as the power-voltage dependence of a CDC in a LV network is typically lower than that of the aggregated models [13].

The key contributions of this paper are as follows:

1) A quantitative comparison between the demand reduction (DR) capabilities of point-of-load voltage control (PVC) against voltage control at substation (VCS) for different time of the day is reported for the first time. Moreover, the rated capacity (and hence, the physical size and capital investment) of the voltage compensators to be deployed is evaluated to weigh the benefits against the cost.

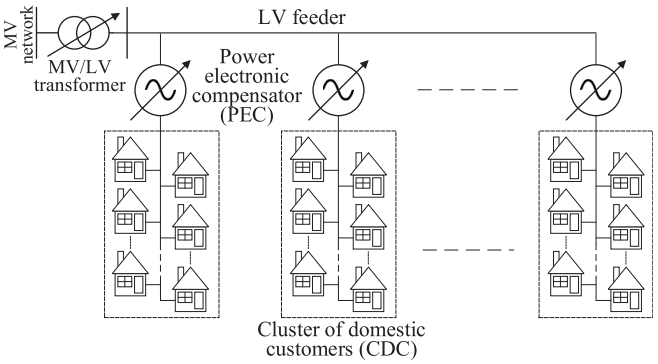

Fig. 1. Point-of-load voltage control (PVC).

2) A high-resolution domestic demand and power-voltage dependence profile at the cluster of domestic customer (CDC) level is used to quantify the voltage-driven demand reduction capability for PVC and VCS. Competing approaches reported in the literature either considered aggregate load models at the medium voltage (MV) level [4] or used load disaggregation at the bulk supply point [12]. Both provide less accurate results compared to the bottom-up approach to voltage-driven demand response adopted in this paper.

The scope of this study is limited to domestic sector only as the necessary high time-resolution demand models for industrial and commercial customers is not readily available.

II. Point-of-Load Voltage Control (PVC)

A. Approach

For point-of-load voltage control (PVC), a cluster of domestic customers (CDC) in close electric proximity could be decoupled from the low voltage (LV) feeder using a power electronic compensator (PEC) as illustrated in Fig. 1. The configuration and size (i.e., number of customers) of each CDC would vary depending on the connection arrangement in a particular feeder. However, the electric proximity should be such that the voltage drop within a CDC is negligible (e.g., less than 1%) compared to that along the LV feeder. As the PEC is connected in series between the feeder and a CDC, it can be rated at only a fraction (typically 5-10%) of the diversified peak demand (DPD) of the CDC. Also, the diversity in demand within each CDC limits the required rating of the PEC.

The supply voltage to each CDC could be controlled independently within the stipulated limits irrespective of the feeder-side voltage subject to the rating of the PEC. This offers more flexibility for demand reduction (and increase, if required) through voltage especially, under high loading conditions as shown in Fig. 2. For illustration purpose, uniform loading of each CDC (which corresponds to each arrow) and equal distance of separation between the CDCs are assumed which result in a linear voltage profile across the feeder. The substation voltage is assumed to be maintained at the maximum stipulated voltage (V_{max}). It is obvious that the extent of voltage reduction using voltage control at substation (VCS) is limited compared to the PVC especially, under high loading condition. The shaded area in Fig. 2 (b) and (d) represents

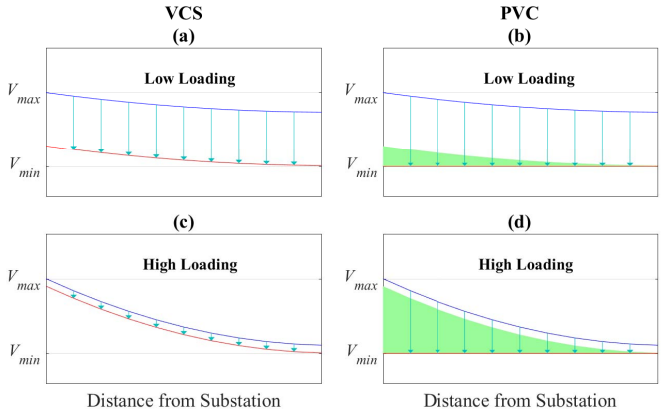

Fig. 2. Possible voltage reduction using (a) and (c) VCS and (b) and (d) PVC in case of low/high loading.

the additional voltage reduction possible with PVC. Alongside the extent of possible voltage reduction, the demand reduction (DR) capability depends on other factors discussed in Section II-B next.

B. Demand Reduction (DR)

The aggregate power-voltage dependence of the ith cluster of domestic customers (CDC) at a given time instant t can be expressed in exponential form [14] as:

$$P_i(t) = P_{i0}(t)V_i(t)^{n_{pi}(t)}, \quad Q_i(t) = Q_{i0}(t)V_i(t)^{n_{qi}(t)} \tag{1}$$

where, $P_{i0}(t)/Q_{i0}(t)$ is the nominal active/reactive power consumption at 1.0 p.u. voltage and $n_{pi}(t)/n_{qi}(t)$ is the aggregate active/reactive power-voltage sensitivity at time t.

As in (1), all the terms in the equations henceforth are time-varying unless otherwise specified. However, to avoid the equations overflowing due to lack of space, the time varying quantities such as $P_{i0}(t), n_{pi}(t)$ would be simply denoted as P_{i0}, n_{pi}.

In a radial distribution feeder, the voltage at ith bus (CDC) could be expressed in terms of the adjacent bus voltage as [15]:

$$V_{Bi}^2 = \left[\left(P_i'R_i + Q_i'X_i - 0.5V_{Bi-1}^2\right)^2 - \left(R_i^2 + X_i^2\right)\left(P_i'^2 + Q_i'^2\right)\right]^{\frac{1}{2}} - \left(P_i'R_i + Q_i'X_i - 0.5V_{Bi-1}^2\right) \tag{2}$$

where

$$P_i' = P_i + \sum_{j=i+1}^{N_c}\left(P_j + P_{LLj}\right), Q_i' = Q_i + \sum_{j=i+1}^{N_c}\left(Q_j + Q_{LLj}\right) \tag{3}$$

where, P_i'/Q_i' sum of the active/reactive power loads at bus i and beyond till the end of the feeder plus sum of the active/reactive power losses in all feeder segments beyond bus i. R_i/X_i is the resistance/reactance of the feeder segment between bus i and $i-1$. With a specified substation voltage V_{B0} the rest of the bus (i.e., CDC) voltages could be worked out for a particular loading condition.

The total active power demand reduction (DR) possible by reducing the voltage of all the CDC to the minimum stipulated limit V_{min} is given by:

$$DR_{PVC} = \sum_{i=1}^{N_c} P_{i0}\left[V_{Bi}^{n_{pi}} - V_{min}^{n_{pi}}\right] - \Delta P_{LL} - \sum_{i=1}^{N_c} P_{LCi} \tag{4}$$

where, N_c is the total number of CDC in the system, ΔP_{LL} represents the change in network power loss as a result of reducing each CDC's voltage to V_{min} and P_{LCi} is the total losses (conduction and switching) incurred in the PEC at CDC i. Typically, network power loss would be less (i.e., ΔP_{LL} is negative) with reduced CDC voltage (and hence, power). The loss in the PEC would depend on the power processed by it (see Section II-C) and its rated capacity. Everything except V_{min} in (4) varies according to the time of the day. For the studies reported subsequently, V_{min} is assumed to be 0.95 p.u. to keep the reduced voltages within acceptable limits which is what the utilities are obliged to ensure. It is to be noted that critical (or sensitive) customers requiring tighter voltage tolerance would not be part of PVC. Such critical customers are generally present in the industrial/commercial sector which is not within the scope of the current study.

For DR through VCS, the total possible active power demand reduction (DR) can be calculated by:

$$DR_{VCS} = \sum_{i=1}^{N_c} P_{i0}\left[V_{Bi}^{n_{pi}} - V_{Bi}'^{n_{pi}}\right] - \Delta P_{LL} \tag{5}$$

where, $V_{Bi}'^{n_{pi}}$ is the reduced feeder-side voltage after VCS, ΔP_{LL} is the change in network power loss as a result of reduced (to V_{Bi}') supply voltage to each CDC.

The DR capabilities of PVC and VCS are compared in terms of an index, ΔDR defined in (6).

$$\Delta DR(\%) = \frac{DR_{VCS} - DR_{PVC}}{DR_{PVC}} \times 100\% \tag{6}$$

In order to obtain a closed form analytical expression for ΔDR, the following simplifying assumptions are made. Relaxing these assumptions would make the derivation of the analytical expression much more complicated.

1) A radial distribution network with N_c uniformly spaced constant current (CI) loads having unity power factor.

2) Purely resistive feeder with a total resistance of R_T (p.u.).

3) The total loading P_T at nominal voltage is uniformly distributed resulting in a current flow $I = P_T/N_c$ through each CI load.

4) PEC losses neglected.

With the substation voltage held at V_S, the voltages of the first three loads are given as:

$$V_{B1} = V_S - N_c I\frac{R_T}{N_c} = V_S - \frac{P_T R_T}{N_c} \tag{7}$$

$$V_{B2} = V_S - (N_c - 1)I\frac{R_T}{N_c} = V_S - \frac{P_T R_T}{N_c}\left(\frac{2N_c - 1}{N_c}\right) \tag{8}$$

$$V_{B3} = V_S - (N_c - 2)I\frac{R_T}{N_c} = V_S - \frac{P_T R_T}{N_c}\left(\frac{3N_c - 3}{N_c}\right) \tag{9}$$

Following this trend, the voltage at i^{th} load can be expressed as (10).

$$V_{Bi} = V_S - \frac{P_T R_T}{N_c^2} i[N_c - 0.5i + 0.5] \tag{10}$$

DR through PVC can then be expressed (11).

$$DR_{PVC} = \sum_{i=1}^{N_c} \frac{P_T}{N_c}[V_{Bi} - V_{min}]$$

$$= P_T(V_S - V_{min}) - \frac{P_T^2 R_T}{6N_c^2}(2N_c + 1)(N_c + 1) \tag{11}$$

It is to be noted that there would be no change in network power losses as all the loads are assumed to be constant current type.

For determining DR through VCS, the minimum possible voltage at the substation V' is obtained such that the voltage at the far end of the feeder is at the minimum limit. The voltages at each node are then recalculated using (10) with V'_S. DR through VCS is given as (12).

$$DR_{VCS} = \sum_{i=1}^{N_c} \frac{P_T}{N_c}[V_{Bi} - V'_{Bi}]$$

$$= P_T(V_S - V_{min}) - \frac{P_T^2 R_T}{2N_c}(N_c + 1) \tag{12}$$

Without loss of generality, N_c is assumed to be 20, V_S maintained at the upper limit 1.05 p.u., and the lower limit V_{min} to be 0.95 p.u. The total feeder resistance R_T is calculated considering violation of the low voltage limit (at the far end of the feeder) beyond a certain amount of overloading (say, 1.2 p.u. loading).

With the above-mentioned assumptions, the variation of ΔDR with respect to loading is shown in Fig. 3 (a). It should be noted that a negative value of ΔDR denotes DR capability of VCS is less than that of PVC according to (6). The advantage of PVC over VCS increases with the loading level. The losses incurred within the PEC have been included numerically as mentioned in Section II-C. PVC provides less DR than VCS at very low loading as the power losses incurred in the PECs become dominant. The traces with $N_c = 5$ and 50 confirm that the impact of varying load density is limited. The absolute values of DR through VCS and PVC are shown in Fig. 3 (b). For a given load type, the DR capability depends of the demand (i.e., loading) itself and is expected to increase (decrease) at higher (lower) loading. However, at higher loading there is less room for voltage (i.e., demand) reduction due to larger voltage drop across the feeder. Due to these opposing trends, the DR capability peaks at a certain loading which is lower for VCS than PVC. This is due to the fact that the room for voltage reduction using VCS becomes lesser than that using PVC with increase in loading level.

The DR capability using PVC under reverse power flow due to photovoltaic (PV) generation is shown in Fig. 3 (b). During reverse power flow, the substation voltage is generally maintained at the minimum limit (0.95 p.u.) to avoid over voltage problem at the far end. It is difficult to continuously adjust the substation voltage with varying PV output which leaves no room for DR through VCS.

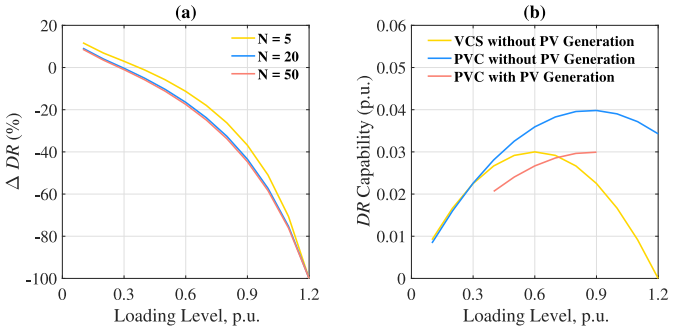

Fig. 3. (a) Variation of ΔDR with loading level under different number of CDCs (b) Variation of DR capability with loading level with/without PV generation.

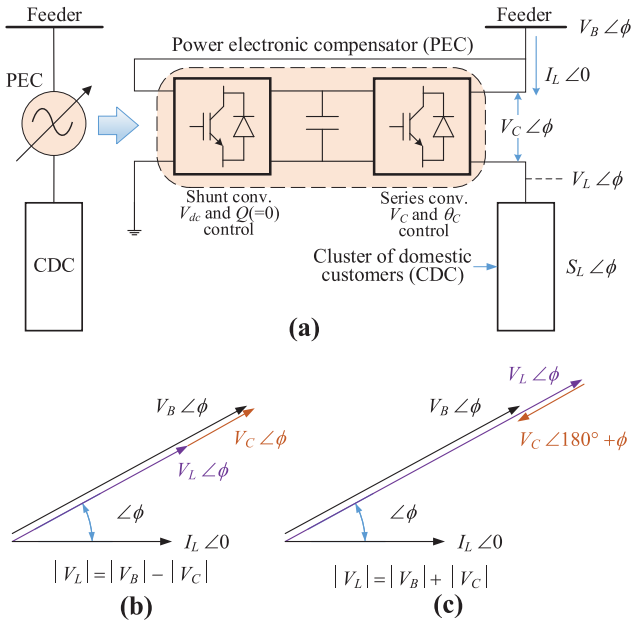

Fig. 4. Power electronic compensator (PEC) for point-of-load voltage control (PVC) (a) configuration; (b) phasor diagram with in phase injected voltage; (c) phasor diagram with out of phase injected voltage.

With PV generation, the range of loading level is limited to 0.4-0.9 p.u. considering the typical variations (shown in Figs 6 & 13) during the daylight hours. The DR capability of PVC is lower in presence of PV generation across different loading levels. This is due to the fact that the substation voltage is generally set at the lower limit 0.95 p.u. to prevent overvoltage at the far end of the feeder which leaves less room for voltage (i.e., demand) reduction compared to the case without PV penetration.

Although the analysis presented above assumes purely resistive feeder and constant current loads only, it provides a theoretical basis for the ΔDR figures obtained later in Sections III and IV using realistic network parameters and high-resolution domestic demand models.

C. Power Electronic Compensator (PEC)

A power electronic compensator (PEC) with back-to-back configuration [16] is used to inject a controllable series voltage between the cluster of the domestic customers (CDC) and the LV feeder. The configuration is shown in Fig. 4(a).

The series converter is set to control both the magnitude (V_C) and phase angle (ϕ) of the injected voltage while the shunt converter is controlled to maintain the DC link voltage supporting the active power exchanged by the series converter. To minimize its apparent power rating, the shunt converter is operated at unity power factor.

For PVC, the magnitude of the injected voltage V_C can be controlled according to the demand reduction (or increase) requirement and the phase angle ϕ is set to be either in or out (to increase demand, if required) of phase with the feeder-side (V_B) or CDC (V_L) voltage (as shown in the phasor diagrams in Fig. 4 (b) and (c)) to exercise maximum change in CDC voltage with minimum apparent power rating. As a result, the PEC exchanges both active and reactive power. For demand reduction, the injected voltage would be in phase with V_B resulting in the series converter absorbing active power and the shunt converter injecting this power back into the feeder. Neglecting the converter losses, the total demand reduction would be equal to the reduction in power consumption of the CDC [17]. Under normal condition, the PEC injects zero voltage ($V_C = 0$) which makes the feeder-side and CDC voltages the same ($V_B = V_L$) neglecting the small voltage drop across the series element of the converter interface filter (not shown explicitly in the figure).

The apparent power processed by the PEC at ith CDC can be expressed as:

$$\begin{aligned} S_{Ci} &= V_{Ci} I_{Li}\left(1 + pf_i'\right) \\ &= \left(V_{Bi}' - V_{min}\right)\sqrt{P_{i0}^2 V_{min}^{2(n_{pi}-1)} + Q_{i0}^2 V_{min}^{2(n_{qi}-1)}}\left(1 + pf_i'\right) \end{aligned} \tag{13}$$

where, V_{Bi}', pf_i' are the modified feeder-side voltage (recalculated from power flow) and power factor, respectively as a result of reduction in voltage of the ith CDC to V_{min}. Apart from the series voltage (V_{Ci}) inserted by the PEC and the CDC current I_{Li} (which is the same as PEC current), the term $(1 + pf_i')$ accounts for the fact that the shunt converter operates at unity power factor while balancing the active power exchanged by the series converter. For the studies reported in Sections III–V, the conduction loss is considered to be 3.75% of the power processed by the PEC while the switching loss is 0.25% of its rated capacity [18]. To avoid additional power loss, the PEC would be bypassed when DR is not exercised. Typically, V_{Bi}' would be slightly larger than V_{Bi} due to decreased feeder voltage drop following CDC voltage (and hence power) reduction.

For a given power consumption $S_i = \sqrt{P_{i0}^2 + Q_{i0}^2}$ by a CDC, the apparent power processed by the PEC (S_{Ci}) is larger when the power-voltage exponents n_{pi}/n_{qi} are smaller. Fortunately, there is a correlation between the actual power consumption of a CDC and the values of the power-voltage exponents with both becoming low/high around similar time of the day. Hence, the power processed by the PEC is always limited. The rating of the PEC to be installed at each CDC would be dictated by the maximum possible S_{Ci} over the 24-hour period and across different seasons (winter/summer) and days (weekdays/weekends).

The total demand reduction possible through PVC at a given time and the rated capacity of the PEC depends on the aggregate demand and power-voltage dependence of each CDC and the voltage across a CDC, all of which vary depending on the time of the day. The voltage also depends on the location of a particular CDC on the feeder. In the subsequent sections, a high resolution domestic demand model is used to quantify the demand reduction with PVC and the PEC rating required first with a random distribution of CDC mimicking a generic LV feeder (Section III) and then with the Cigre benchmark MV/LV network (Section IV).

III. Generic Low Voltage (LV) Feeder

The demand reduction (DR) capability of PVC depends on the feeder configuration and the loading profile. In this section, the DR of PVC is compared against that of voltage control at substation (VCS) using a generic LV feeder with random separation between adjacent CDCs and random distribution of loads among the CDCs. A stochastic demand model for domestic customers in Great Britain is considered. The case studies presented in this and subsequent sections are performed in MATLAB running on Intel(R) E5-1650 v3 3.5GHz PC.

A. Domestic Demand Model

The 24-hour demand profile for each domestic customer is generated using a domestic demand model developed by the Centre for Renewable Energy Systems Technology (CREST) [19]. The model provides household level electricity consumption with one minute resolution by allocating the usage of 35 typical household appliances according to daily activity and active occupancy pattern for a given number of residents, day of the week and month of the year. A set of 24-hour total demand profiles for each appliance (P_d) and individual domestic customers (P_h) are obtained by running the demand model repeatedly. Combining these demand profiles with the ZIP load model coefficients (Z_p, I_p, P_p) of the 35 appliances [20], the aggregate active power-voltage sensitivity (n_{ph}) for each domestic customer is calculated by:

$$n_{ph} \approx \frac{\sum_{i=1}^{35} P_{di}\left(2 \times Z_{pi} + 1 \times I_{pi} + 0 \times P_{pi}\right)}{\sum_{i=1}^{35} P_{di}\left(Z_{pi} + I_{pi} + P_{pi}\right)} \tag{14}$$

Then the aggregate active power-voltage sensitivity at the i^{th} CDC, which is used to determine the DR capability, is obtained by (15) in which N_h is the number of domestic customers within a CDC.

$$n_{pi} \approx \frac{\sum_{k=1}^{N_h} P_{hk} \times n_{phk}}{\sum_{k=1}^{N_h} P_{hk}}. \tag{15}$$

B. Demand Reduction (DR) Capability

To compare the DR capability of PVC and VCS, a generic radial LV feeder with random distribution of loads among

TABLE I
PARAMETER RANGE FOR DEMAND REDUCTION CALCULATION

Parameter	Range
Total diversified peak demand (P_T)	0.5 - 1.5 p.u.
Number of CDC (N_c)	5 - 20
Loading of each CDC	$0.5P_T/N_c$ - $1.5P_T/N_c$
Length of feeder segments	$0.5Z_f/N_c$, $1.5Z_f/N_c$

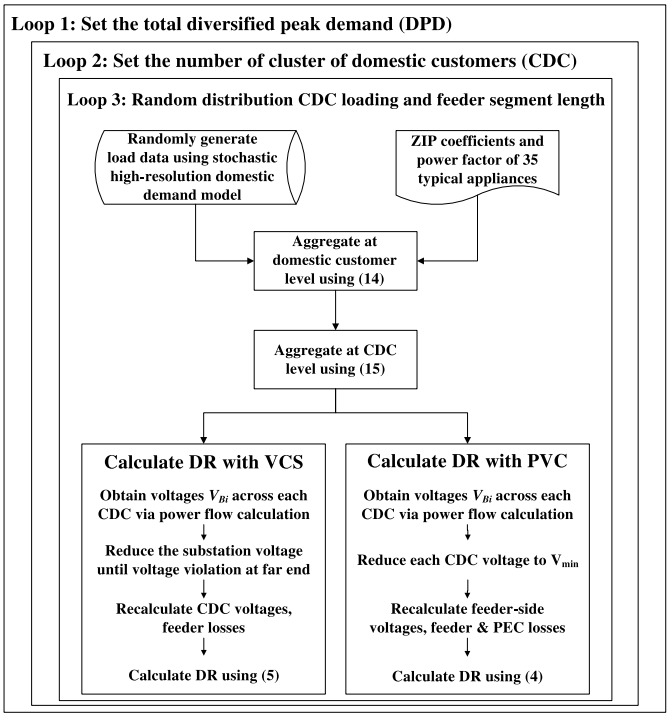

Fig. 5. Calculation of demand reduction capability.

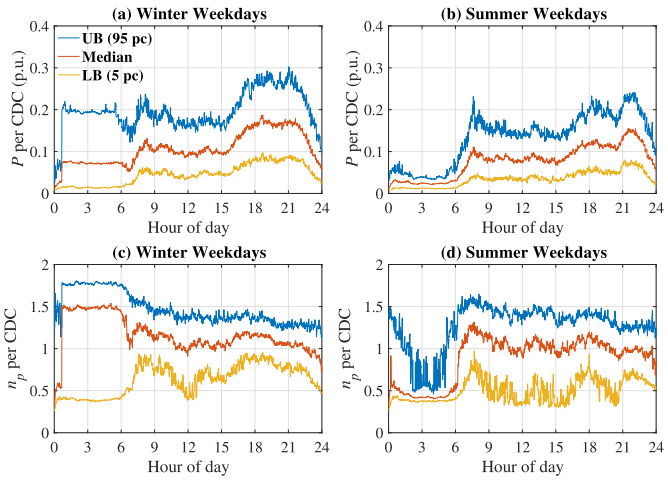

Fig. 6. Aggregate active power consumption and active power-voltage exponent at CDCs for (a) and (c) winter and (b) and (d) summer weekdays.

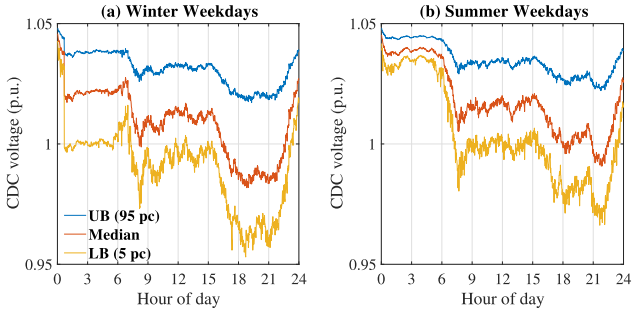

Fig. 7. Voltage across CDCs for (a) winter and (b) summer weekdays.

CDC and random length of feeder sections is considered to obtain a general range of possible ΔDR under various network configurations. A fixed length (Z_f) and typical line parameters [21] of the LV feeder are considered while the number of CDC is varied between 5 and 20. The loading of each CDC and the length of each feeder segment (between adjacent CDCs) are varied randomly between ±50% of their values corresponding to an uniform distribution. The total diversified peak demand (DPD) of the feeder is also varied between ±50% of the nominal value. These are summarized in Table I.

The DR capability is calculated by looping through the variation in the above parameters as shown in Fig. 5. Starting from the outer loop, Loop 1, 2 and 3 varies the total DPD of the entire feeder, the number of CDC and distribution of loading between them, respectively. This encompasses a wide range of LV feeder configurations including a dense urban or a spare rural network. The upstream MV network is represented by its Thevenin equivalent.

The results shown in Figs. 6 to 9 correspond to typical winter and summer weekdays. A fixed total DPD (1.0 p.u.) and number of CDCs are considered to filter out the trends. Each figure consists of three traces representing the upper boundary (UB, 95 percentile), median value (50 percentile) and lower boundary (LB, 5 percentile) of the results considering the variations.

Fig. 6 shows the 24-hour variation of active power consumption (P) and active power-voltage exponent (n_p) aggregated at the CDC level. The three traces show the variability in P, n_p between different CDCs. The UB of P is nearly 3 times the LB which corresponds to the range set in Table I. The DPD across the day is larger for winter weekdays than summer with a prominent effect of electric heating (higher P and n_p) during the winter nights.

The time variation of voltage across the CDCs, shown in Fig. 7, is consistent with the loading of CDC in Fig. 6. The three traces in CDC voltage profiles represent the variability due to different electric proximity to the substation. It is to be noted that the MV/LV transformer secondary tap position is maintained at 1.05 p.u. to avoid under-voltage at the far end of the feeder.

Fig. 8 shows the DR capability of PVC and ΔDR for typical winter and summer weekdays. As mentioned before, a negative value of ΔDR denotes DR capability of VCS is less than that of PVC according to (6). During the winter weekdays, DR capability of PVC varies between 2% to 7% of the DPD across the 24-hour period. The DR capability of VCS is 40% to 55% less during most part (around 22:00-17:00 hours) of the day. During peak demand hours (around 17:00 - 22:00), the DR capability of VCS is much less with ΔDR touching -100%

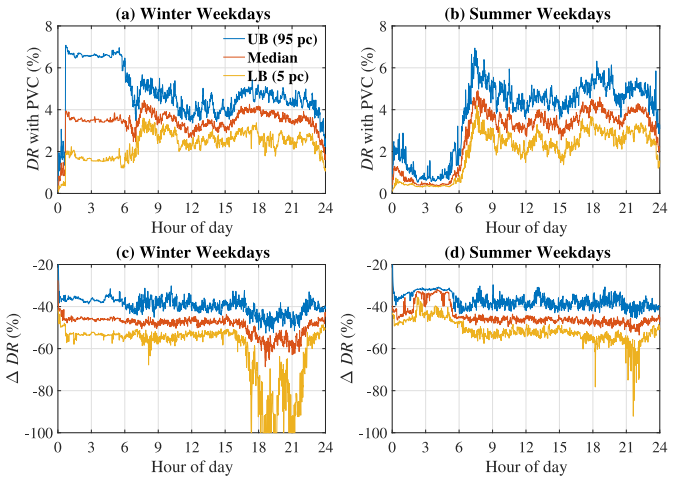

Fig. 8. Demand reduction (DR) capability of PVC and comparison with that of VCS (ΔDR) for (a) and (c) winter and (b) and (d) summer weekdays.

in some cases. This denotes that VCS totally loses its DR capability as the voltage at the far end of the feeder is below the lowest stipulated limit. Without electric heating, the DR capability of PVC would be less during the winter nights but the comparison against VCS (ΔDR) would still be similar.

For summer weekdays, the maximum capability of PVC is around 6% while the minimum can be as low as around 0.5% due to the very light loading during the late night and early hours of the day. The capability of VCS for other time of the day is still around 40% to 55% less except some instances during the late evening peak where DR with VCS could be up to about 80% less.

C. PEC Power

Improved DR capability of PVC comes at the expense of requirement of power electronic compensators (PECs) at each CDC. Fig. 9 shows the variations in the total apparent power processed by the PECs to achieve the DR shown in Fig. 6. This is expressed as a percentage of the diversified peak apparent power demand of the feeder. Overall, about 2-12% of the power is processed by the PECs although the power through a particular PEC would depend on the loading level and active power-voltage exponent. It is interesting to note that during winter night hours, PVC offers higher DR capability with less power through PEC. This is due to relatively less loading (i.e., higher voltages) and higher power-voltage exponent as discussed earlier in Section II-C. The data points close to the upper bound (UB) trace correspond to the CDCs located close to the MV/LV transformer while those near the lower bound (LB) trace are CDCs at the far end of the feeder. The rating of each PEC is decided based on their individual maximum power processed over a range of winter and summer days as clarified further in Section IV.

D. Sensitivity Analysis

The impact of varying loading and different number of CDCs connected to the feeder is considered here.

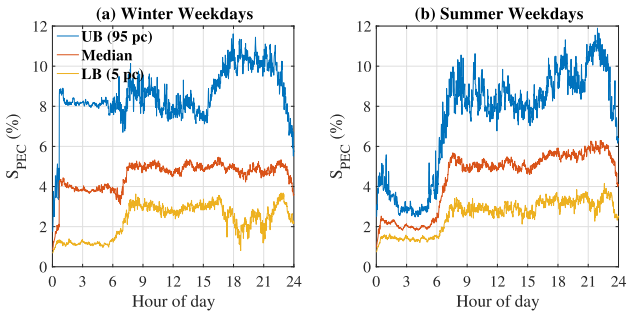

Fig. 9. Total apparent power processed by the power electronic compensators (PECs) for (a) winter and (b) summer weekdays.

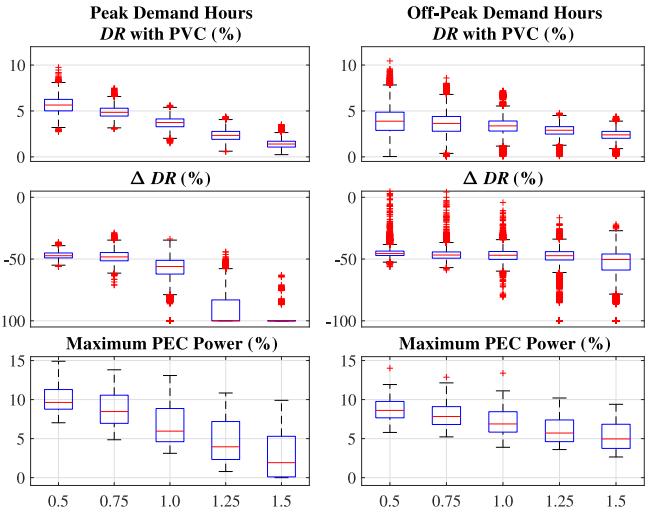

Fig. 10. Impact of loading level on demand reduction (DR) capability and PEC rating required.

1) Loading Condition: The total DPD of the feeder is varied between ±50% of the nominal value to capture the impact of loading on DR capability of PVC.

Fig. 10 shows the results for peak (17:00-22:00) and off-peak (22:00-17:00) demand hours for winter weekdays. Although the DR capability of PVC reduces with higher loading, its effectiveness over VCS (ΔDR) actually increases. In fact, VCS would totally lose its DR capability for most part of the peak hours when the loading is high.

The sum of the maximum power processed by individual PECs connected at various CDCs are shown in Fig. 10 for peak and off-peak demand hours separately. The PEC power is less for higher loading due to the reasons mentioned above.

2) Number of CDC: The number of CDCs served by the LV feeder is varied between 5 to 20 keeping the total DPD fixed at 1.0 p.u. For a fixed loading, the voltage drop across the feeder is expected to be less for higher number of CDCs resulting in reduced difference between the DR capability of PVC and VCS. This trend could be observed in Fig. 11. For 15 or 20 CDCs, in some instances (as shown by the outliers) VCS offers similar (or even higher) DR capability as PVC during the off-peak demand hours. However, the impact of varying the number of CDCs numbers is not as significant as changing

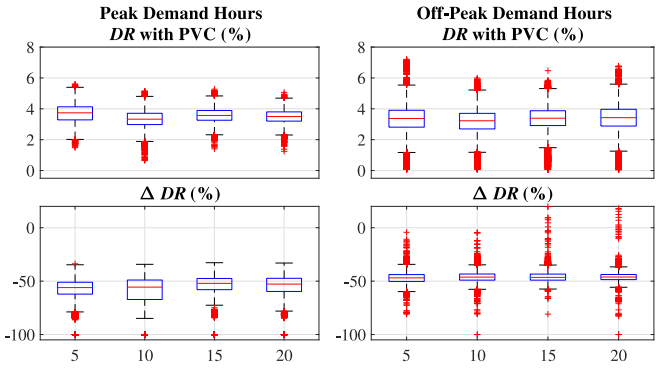

Fig. 11. Impact of number of CDCs on demand reduction (DR) capability.

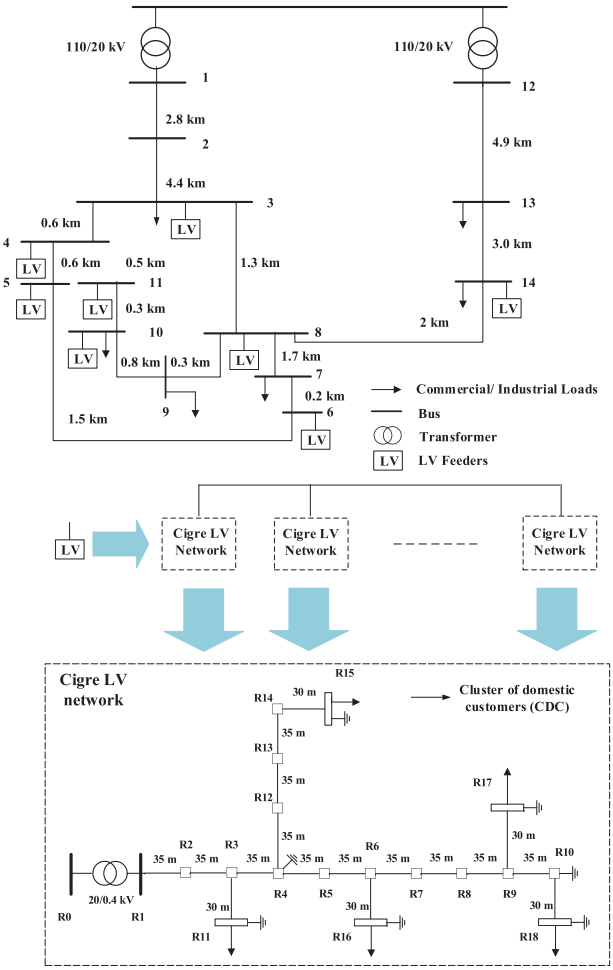

Fig. 12. Cigre LV/MV benchmark network.

the loading level which is consistent with the analysis provided in Section II-B.

IV. Cigre Benchmark MV/LV Network

A. Network Description

The Cigre European benchmark medium- and low-voltage (MV/LV) network [22] shown in Fig. 12 is considered in this section to further validate the general range of ΔDR achieved from the generic LV feeder in Section III. The aggregated load at each MV bus is split into commercial/industrial loads

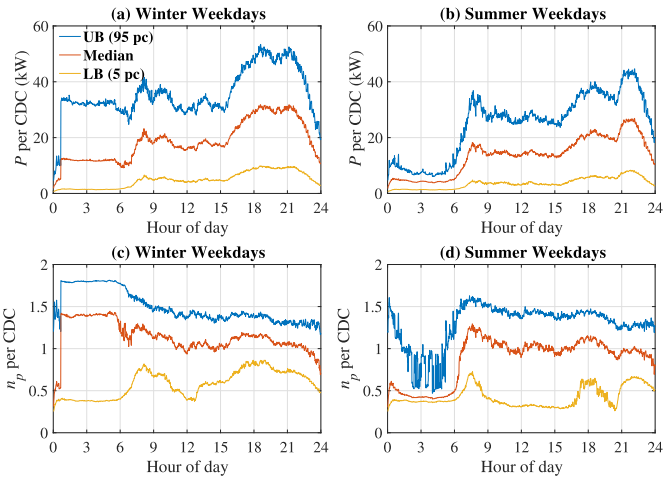

Fig. 13. Aggregate active power consumption and active power-voltage exponent at CDCs for (a) and (c) winter and (b) and (d) summer weekdays.

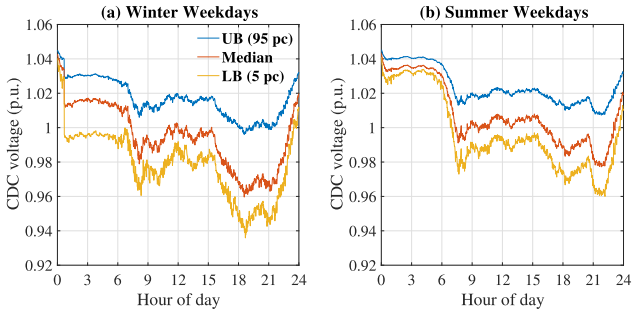

Fig. 14. Voltage across CDCs for (a) winter and (b) summer weekdays.

and multiple parallel Cigre benchmark LV feeders each containing 5 cluster of domestic customers (CDCs). The number of domestic customers connected at R11, R15-R18 are 14, 47, 50, 32, 42, respectively based on the DPD in [22]. The total DPD is 5.5 MVA with 70% domestic loads connected to the LV feeders and 30% commercial/industrial loads at the MV level [22]. As a high-resolution demand model (such as in [19]) for commercial and industrial customers is not readily available, the power-voltage dependence of only the domestic customers is considered for this study to ensure a fair comparison between PVC and VCS.

The aggregated active power consumption (P) and the corresponding active power-voltage exponent (n_p) of the CDCs for winter and summer weekdays are shown in Fig. 13. As in Section III, these are obtained from the high-resolution domestic demand model [19]. The traces denote the upper boundary (UB, 95 percentile), median value (50 percentile) and lower boundary (LB, 5 percentile) of the results.

The voltages across CDCs, show in Fig. 14, are relatively low compared to the case study with a generic LV feeder in Section III. This is evident during 1) winter peak hours (17:00 - 22:00) (in some cases below 0.95 p.u.) due to a higher loading condition and 2) daytime (around 8:00 - 15:00) due to the presence of commercial/industrial loads at the MV level.

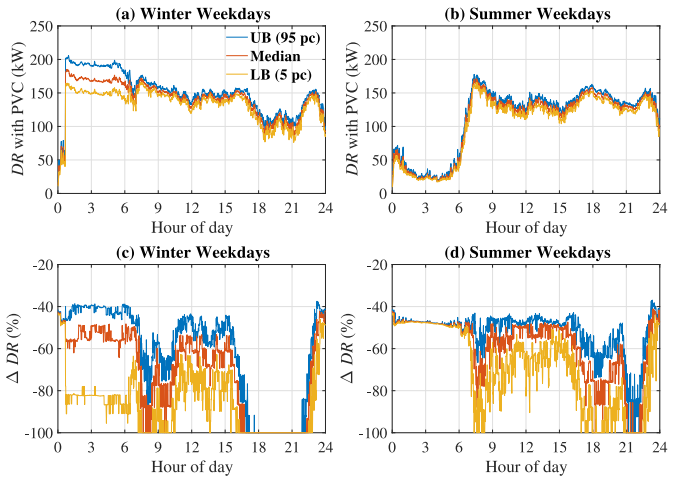

Fig. 15. Demand reduction (DR) capability of PVC and comparison with that of VCS (ΔDR) for (a) and (c) winter and (b) and (d) summer weekdays.

B. Demand Reduction (DR) Capability

The DR capability of PVC and VCS are compared in Fig. 15. PVC can provide a DR of 100kW to 180kW depending on the time of the day for both winter and summer weekdays. Variation of DR capability throughout a day is similar to that in Section III but with a smaller difference between UB and LB due to a fixed network configuration here unlike the generic LV feeder in Section III. In practice, the system operators could rely on the LB of the DR capability as this amount of DR is 'very likely' to be available even after considering all the variabilities.

The DR capability of VCS is significantly less (lower negative values of ΔDR) for the Cigre benchmark MV/LV network compared to the generic LV feeder which is mainly due to relatively low CDC voltage as a result of higher loading. During the peak demand hours, VCS cannot produce any DR as the voltage at the far end of certain LV feeder(s) violates the stipulated lower limit. During other times of the day, the DR capability of VCS is also limited due to large voltage drops caused by the commercial/industrial loads. For instance, when the commercial/industrial loads peak between 8-9 am [22], the DR capability of VCS is virtually zero. The LV feeders are connected to the MV network (bus 3-6, 8, 10-11 and 14) at different electrical distances from the primary (110/20 kV) substation. This leads to a much wider range of ΔDR as compared to the previous section where a fixed equivalent impedance was used to represent the MV network.

C. PEC Rating

The rated capacity of the PEC required at each CDC is determined by the maximum power processed. These are shown in Fig. 16 separately for each bus (R11, R15-R18) considering all the 31 LV feeders with a total of 155 CDCs. The CDCs at R16 of all the LV feeders require a larger PEC rating due to high DPD and relatively small electrical distance from the MV/LV transformer. The rating of the PECs at different CDCs vary between 2-5 kVA which is less than 10% of the DPD of the respective CDC.

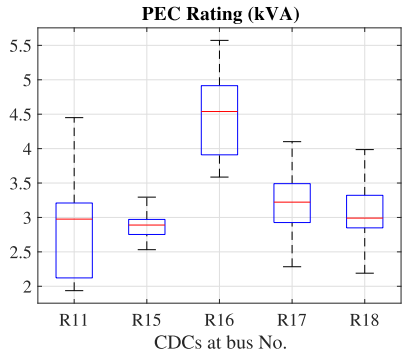

Fig. 16. Rating of power electronic compensators (PECs) at different buses across all the LV feeders with 155 clusters of domestic customers (CDCs).

The total rated capacity of the PECs required for the Cigre MV/LV network is around 500 kVA. Considering a conservative figure of \$150/kVA [23] for a typical low voltage single phase converter, the investment in deploying the PECs would be around \$75K. This could be recovered by utilizing the DR capability of PVC to reduce the conventional operating reserve (OR) requirement and thus, decrease the OR availability (or holding) fees and OR utilization fees paid to conventional OR providers. The saving in OR utilization fees depends on the actual balancing requirements of the system which varies with the proportion of intermittent renewable generation, available storage capacity etc. Summing up the hourly average of lower bound of DR capability of PVC (shown in Fig. 15 (b) and (c)) for various days (summer, winter, weekdays, weekends), the total yearly DR capability turns out to be 1030 MWh. Considering an OR holding fee of £6/MW/h [24] (although this varies depending on market condition) the payback period for the investment in PECs would be around 8-9 years using the current exchange rate of £1=\$1.4. Note that this is based on the saving in OR holding fee only. The actual payback period would be considerably less once the saving in OR utilization fee is factored into the calculation using the projected scenarios. This is because the OR utilization fee is typically much higher (e.g., £150/MW/h) and volume and frequency of OR utilization will increase with large penetration of intermittent renewable energy sources.

V. Frequency Control in Islanded Microgrid

The frequency control problem in an islanded microgrid is considered in this section to illustrate the effectiveness of the DR capability of PVC. Recently, [25] showed that frequency regulation through generator voltage control (GVC) (which is analogous to VCS in this context) in an islanded microgrid could facilitate integration of significant levels of intermittent renewable resources without energy storage. Variations of active power-voltage exponents (n_p, n_q) throughout the day were not considered in [25]. The frequency control capability of PVC is benchmarked against the GVC approach [25].

In islanded condition, the Cigre benchmark MV/LV microgrid (shown in Fig. 12) is supplied by two 2.3 MVA diesel generators at bus 1 and 12. Each generator is represented by a third-order dynamic model with the parameters given

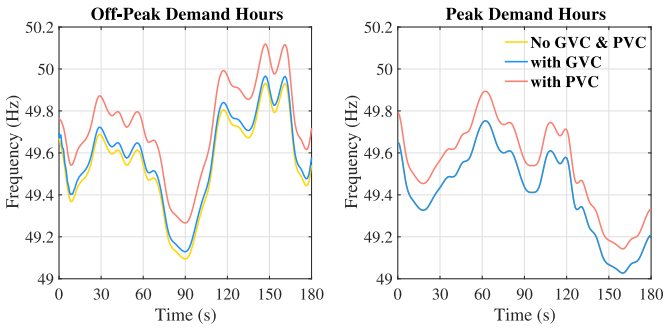

Fig. 17. Dynamic variation of microgrid frequency.

in [26]. The standard IEEE-DC1A type excitation system and simple first order model for the governor with 5% power-frequency droop are used. The wind power generation with a rated capacity of 1.5 MW at bus 7 operates under maximum power capture mode while maintaining unity power factor at its point of connection to the microgrid. Similar fluctuation of wind power but with higher amplitude than [25] is considered to cause larger frequency excursions. The simulations are carried out in MATLAB/Simulink with a minimum step size of 0.01s. Fig. 17 shows two 3-minute time windows from off-peak and peak demand hours which confirm that DR through PVC is able to regulate the microgrid frequency better than GVC. During peak demand hours, the trace with GVC overlaps with that without frequency control (No GVC & PVC) as GVC cannot improve (i.e., reduce) the frequency excursion at all due to voltage limit violation at the far end of certain LV feeders. Besides, GVC produces only marginal improvement even during off-peak demand hours. The simulation results correspond to the DR capability shown in IV-B and highlight the effectiveness of DR through PVC.

VI. Conclusion

Recent trials in Great Britain have shown that up to about 3 GW of system wide demand reduction (DR) is possible through voltage control at (primary) substation (VCS) alone. This paper confirms that such a large DR using VCS might not be possible under high loading. The DR capability of VCS is found to be 40-60% lower than that of point-of-load voltage control (PVC) for most part of the day and even less (up to 100% less) during the peak demand hours. Higher DR with PVC is achieved with power electronic compensators (PEC) rated at only about 10% of the diversified peak demand resulting in a reasonable payback time on investment. A high resolution domestic demand model, a generic LV feeder and a Cigre benchmark network are considered to generalize and substantiate the above findings. As a possible application, DR through PVC is shown to produce better frequency control in an islanded microgrid with fluctuating wind power generation.

In future, loading of distribution networks would increase drastically during certain times of the day due to rise in distributed generation (e.g., roof-top solar) and electrification of heat and transport. During these periods, DR capability of VCS would be seriously limited (even becoming zero) necessitating PVC as demonstrated in this paper. Use of PVC would reduce the need for operating reserve from various sources (e.g., energy storage etc.) and thereby, facilitate large-scale integration of intermittent renewable energy sources such as wind and solar power.

Acknowledgment

The authors would like to thank Dr. Diptargha Chakravorty for his help in building up the domestic demand model. Supporting data is available on request. Please contact cap-publications@imperial.ac.uk.

References

[1] A. Losi, P. Mancarella, and A. Vicino, *Integration of Demand Response Into the Electricity Chain: Challenges, Opportunities and Smart Grid Solutions*. Hoboken, NJ, USA: Wiley, 2015.

[2] S. H. Tindemans, V. Trovato, and G. Strbac, "Decentralized control of thermostatic loads for flexible demand response," *IEEE Trans. Control Syst. Technol.*, vol. 23, no. 5, pp. 1685–1700, Sep. 2015.

[3] K. P. Schneider, F. K. Tuffner, J. C. Fuller, and R. Singh. (2010). *Evaluation of Conservation Voltage Reduction (CVR) on a National Level*. [Online]. Available: https://www.pnnl.gov/main/publications/external/technical_reports/PNNL-19596.pdf

[4] A. Ballanti and L. F. Ochoa, "Voltage-Led load management in whole distribution networks," *IEEE Trans. Power Syst.*, vol. 33, no. 2, pp. 1544–1554, Mar. 2018.

[5] Y. Zheng, D. J. Hill, K. Meng, and S. Y. Hui, "Critical bus voltage support in distribution systems with electric springs and responsibility sharing," *IEEE Trans. Power Syst.*, vol. 32, no. 5, pp. 3584–3593, Sep. 2017.

[6] S. Y. Hui, C. K. Lee, and F. F. Wu, "Electric springs—A new smart grid technology," *IEEE Trans. Smart Grid*, vol. 3, no. 3, pp. 1552–1561, Sep. 2012.

[7] X. Luo *et al.*, "Distributed voltage control with electric springs: Comparison with STATCOM," *IEEE Trans. Smart Grid*, vol. 6, no. 1, pp. 209–219, Jan. 2015.

[8] X. Chen, Y. Hou, and S. Y. R. Hui, "Distributed control of multiple electric springs for voltage control in microgrid," *IEEE Trans. Smart Grid*, vol. 8, no. 3, pp. 1350–1359, May 2017.

[9] Z. Akhtar, B. Chaudhuri, and S. Y. R. Hui, "Primary frequency control contribution from smart loads using reactive compensation," *IEEE Trans. Smart Grid*, vol. 6, no. 5, pp. 2356–2365, Sep. 2015.

[10] S. Yan, S.-C. Tan, C.-K. Lee, B. Chaudhuri, and S. Y. R. Hui, "Use of smart loads for power quality improvement," *IEEE J. Emerg. Sel. Topics Power Electron.*, vol. 5, no. 1, pp. 504–512, Mar. 2017.

[11] D. Chakravorty, B. Chaudhuri, and S. Y. R. Hui, "Rapid frequency response from smart loads in great Britain power system," *IEEE Trans. Smart Grid*, vol. 8, no. 5, pp. 2160–2169, Sep. 2017.

[12] D. Chakravorty, B. Chaudhuri, and S. Y. R. Hui, "Estimation of aggregate reserve with point-of-load voltage control," *IEEE Trans. Smart Grid*, vol. 9, no. 5, pp. 4649–4658, Sep. 2018.

[13] A. J. Collin, G. Tsagarakis, A. E. Kiprakis, and S. McLaughlin, "Development of low-voltage load models for the residential load sector," *IEEE Trans. Power Syst.*, vol. 29, no. 5, pp. 2180–2188, Sep. 2014.

[14] P. Kundur, N. J. Balu, and M. G. Lauby, *Power System Stability and Control*, vol. 7. New York, NY, USA: McGraw-Hill, 1994.

[15] D. Das, D. P. Kothari, and A. Kalam, "Simple and efficient method for load flow solution of radial distribution networks," *Int. J. Elect. Power Energy Syst.*, vol. 17, no. 5, pp. 335–346, 1995.

[16] S.-C. Tan, C. K. Lee, and S. Y. Hui, "General steady-state analysis and control principle of electric springs with active and reactive power compensations," *IEEE Trans. Power Electron.*, vol. 28, no. 8, pp. 3958–3969, Aug. 2013.

[17] Z. Akhtar, B. Chaudhuri, and S. Y. R. Hui, "Smart loads for voltage control in distribution networks," *IEEE Trans. Smart Grid*, vol. 8, no. 2, pp. 937–946, Mar. 2017.

[18] [Online]. Available: http://www.gosolarcalifornia.ca.gov/equipment/inverters.php

[19] I. Richardson, M. Thomson, D. Infield, and C. Clifford, "Domestic electricity use: A high-resolution energy demand model," *Energy Build.*, vol. 42, no. 10, pp. 1878–1887, 2010.

[20] A. Ballanti and L. Ochoa. (2015). *WP2 Part A—Final Report 'Off-Line Capability Assessment.'* [Online]. Available: https://www.nationalgrid.com/sites/default/files/documents/SOF%20-%20LFDD%20-%20July%202017.pdf
[21] "Modeling and aggregation of loads in flexible power networks," Cigre, Paris, France, Rep. 5, Feb. 2014.
[22] "Benchmark systems for network integration of renewable and distributed energy resources," Cigre, Paris, France, Rep. TF C6.04, Apr. 2014.
[23] R. Fu *et al.*, "U.S. solar photovoltaic system cost benchmark: Q1 2017," NREL, Golden, CO, USA, Rep. NREL/TP-6A20-68925, Sep. 2017.
[24] National Grid. (2017). *STOR Annual Market Report 2016–2017 Data*. [Online]. Available: https://www.nationalgrid.com/uk/electricity/balancing-services/reserve-services/short-term-operating-reserve-stor?market-information
[25] M. Farrokhabadi, C. A. Cañizares, and K. Bhattacharya, "Frequency control in isolated/islanded microgrids through voltage regulation," *IEEE Trans. Smart Grid*, vol. 8, no. 3, pp. 1185–1194, May 2017.
[26] K. E. Yeager and J. R. Willis, "Modeling of emergency diesel generators in an 800 megawatt nuclear power plant," *IEEE Trans. Energy Convers.*, vol. 8, no. 3, pp. 433–441, Sep. 1993.

Jinrui Guo (S'16) received the B.Sc. and M.Sc. degrees from North China Electric Power University, Beijing, China, in 2012 and 2015, respectively. He is currently pursuing the Ph.D. degree with Imperial College London, U.K. His research interests include power system stability, smart grid, and renewable energy integration.

Balarko Chaudhuri (M'06–SM'11) received the Ph.D. degree in electrical and electronic engineering from Imperial College London, London, U.K., in 2005, where he is currently a Reader in power systems with the Control and Power Research Group. His research interests include power systems stability, grid integration of renewables, HVDC, FACTS, demand response, and smart grids. He is an Editor of the IEEE TRANSACTIONS ON SMART GRID and an Associate Editor of the IEEE SYSTEMS JOURNAL and Elsevier *Control Engineering Practice*. He is a fellow of the Institution of Engineering and Technology and a member of the International Council on Large Electric Systems (CIGRE).

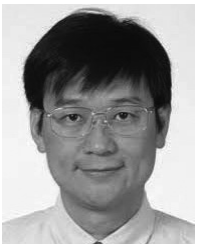

Shu Yuen Ron Hui (M'87–SM'94–F'03) received the B.Sc. degree (Hons.) in electrical and electronic engineering from the University of Birmingham, Birmingham, U.K., in 1984, and the D.I.C. and Ph.D. degrees from Imperial College London, London, U.K., in 1987. He currently holds the Philip Wong Wilson Wong Chair Professorship with the University of Hong Kong, Hong Kong. Since 2010, he has been concurrently held a part-time Chair Professorship in Power Electronics with Imperial College London. He has published over 200 technical papers, including about 170 refereed journal publications and book chapters. Over 55 of his patents have been adopted by industry. He was a recipient of the IEEE Rudolf Chope Research and Development Award from the IEEE Industrial Electronics Society and the IET Achievement Medal (Crompton Medal) from the Institution of Engineering and Technology in 2010 and the 2015 IEEE William E. Newell Power Electronics Award. He is an Associate Editor of the IEEE TRANSACTIONS ON POWER ELECTRONICS and the IEEE TRANSACTIONS ON INDUSTRIAL ELECTRONICS. He is a fellow of the Australian Academy of Technological Sciences and Engineering.